

Stability analysis of an implicit and explicit numerical method for Volterra integro-differential equations with kernel $K(x, y(t), t)$

J. S. C. Prentice
 Senior Research Officer
 Mathsophical Ltd.
 Johannesburg, South Africa
 Email: jpmsro@mathsophical.com

June 23, 2023

Abstract

We present implicit and explicit versions of a numerical algorithm for solving a Volterra integro-differential equation. These algorithms are an extension of our previous work, and cater for a kernel of general form. We use an appropriate test equation to study the stability of both algorithms, numerically deriving stability regions. The region for the implicit method appears to be unbounded, while the explicit has a bounded region close to the origin. We perform a few calculations to demonstrate our results.

1 Introduction

Recently, we described a numerical method for solving the Volterra integro-differential equation

$$y^{(n)}(x) = f(x, y) + \int_{x_0}^x K dt, \quad x > x_0 \quad (1)$$

with various specific forms for the kernel K [1]. In this paper, a sequel to [1], we consider the more general kernel

$$K = K(x, y(t), t).$$

We modify our previous algorithm appropriately, and we consider both implicit and explicit forms of the resulting algorithm. Our attention will primarily be focussed on the stability of these algorithms.

2 Algorithm

To begin with, we consider the case of $n = 1$ in (1). We describe the more general case in Appendix B. We partition the interval of interest, denoted $[x_0, x_N]$, by means of the *equispaced* nodes

$$x_0 < x_1 < x_2 < \dots < x_N. \quad (2)$$

The spacing between the nodes - the *stepsize* - is denoted h .

Using the initial value

$$y(x_0) = y_0,$$

we compute the solution at x_1 via

$$\begin{aligned} y_1 &= y_0 + hf(x_1, y_1) + h \int_{x_0}^{x_1} K(x_1, y(t), t) dt \\ &= y_0 + hf(x_1, y_1) + h \left(\frac{h}{2} \right) (K(x_1, y_0, x_0) + K(x_1, y_1, x_1)), \end{aligned}$$

and the solution at x_2 via

$$\begin{aligned} y_2 &= y_1 + hf(x_2, y_2) + h \int_{x_0}^{x_2} K(x_2, y(t), t) dt \\ &= y_1 + hf(x_2, y_2) \\ &\quad + \frac{h^2}{2} (K(x_2, y_0, x_0) + 2K(x_2, y_1, x_1) + K(x_2, y_2, x_2)). \end{aligned}$$

In both cases, the integral has been approximated using the composite Trapezium Rule with values for t obtained from the nodes. It must be appreciated that, because the kernel is dependent on x_i - the upper limit of the integral - the integral must be calculated in its entirety at each iteration. Hence, there will be an increasing number of terms in the Trapezium approximation as the iteration proceeds.

In general we have

$$\begin{aligned} y_{i+1} &= y_i + hf(x_{i+1}, y_{i+1}) + h \int_{x_0}^{x_{i+1}} K(x_{i+1}, y(t), t) dt \\ &= y_i + hf(x_{i+1}, y_{i+1}) \\ &\quad + \frac{h^2}{2} \left(\sum_{j=0}^{i+1} 2K(x_{i+1}, y_j, x_j) - K(x_{i+1}, y_0, x_0) - K(x_{i+1}, y_{i+1}, x_{i+1}) \right). \end{aligned} \quad (3)$$

The presence of y_{i+1} on both sides identifies this as an *implicit* algorithm. In Appendix B we provide an insight into how this equation can be solved for y_{i+1} using Newton's Method.

The *explicit* form of (3) is given by

$$y_{i+1} = y_i + hf(x_i, y_i) + \frac{h^2}{2} \left(\sum_{j=0}^i 2K(x_i, y_j, x_j) - K(x_i, y_0, x_0) - K(x_i, y_i, x_i) \right). \quad (4)$$

3 Stability

The test equation we use here is

$$y'(x) = \lambda(y - 1) + \gamma \int_0^x y(t) dt \quad (5)$$

$$y(0) = 2$$

with solution

$$y(x) = e^{m_1 x} + e^{m_2 x}$$

$$m_1 = \frac{\lambda - \sqrt{\lambda^2 + 4\gamma}}{2}, \quad m_2 = \frac{\lambda + \sqrt{\lambda^2 + 4\gamma}}{2}$$

when m_1 and m_2 are real ($\lambda^2 + 4\gamma \geq 0$), and

$$y(x) = 2e^{\frac{\lambda x}{2}} \cos\left(x\sqrt{|\lambda^2 + 4\gamma|}\right)$$

when m_1 and m_2 are complex ($\lambda^2 + 4\gamma < 0$). This test equation is similar to that used elsewhere [2][3].

In (5), λ is intended to represent $\partial f/\partial y$ and γ is intended to represent $\partial K/\partial y$. When $\lambda > 0$ and/or $\gamma > 0$, at least one of m_1 and m_2 will also be greater than zero, ensuring that the solution $y(x)$ is an increasing function of x . Note that if $\gamma > 0$, m_1 and m_2 cannot be complex (thus obviating the oscillatory solution), and if $\lambda > 0$ and m_1 and m_2 are complex, then the oscillatory solution has exponentially increasing amplitude. In all of these cases, $|y(x)| \rightarrow \infty$ with x . Only when $\lambda \leq 0$ and $\gamma \leq 0$ do we have the case that $|y(x)| \rightarrow 0$ with x . We acknowledge that when $\lambda = \gamma = 0$, we have the constant solution $y(x) = 2$.

The property of *stability* requires that the numerical solution to the test equation qualitatively mimics the test solution in the sense $|y(x)| \rightarrow 0$ with x . This means that, at the very least, $|y_i| < y(0) = 2$ for all i , when $\lambda < 0$ and $\gamma \leq 0$, and $|y_i| = 2$ when $\lambda = \gamma = 0$.

3.1 Implicit case

The *stability function* for (3) is obtained by applying (3) to the test equation:

$$\begin{aligned} y_1 &= y_0 + h(\lambda(y_1 - 1)) + \left(\frac{\gamma h^2}{2}\right)(y_0 + y_1) \\ &= 2 + zy_1 - z + \frac{w}{2}(2 + y_1) \\ \Rightarrow y_1 &= \frac{2 - z + w}{1 - z - \frac{w}{2}} = 2 \left(\frac{2 - z + w}{2 - 2z - w}\right) \\ &\equiv P_1 = P_1(z, w), \end{aligned}$$

where we have defined $z \equiv h\lambda, w \equiv h^2\gamma$ and P_1 is the stability function at x_1 - i.e. the numerical solution of the test equation at x_1 . It can be shown that

$$P_i = P_i(z, w) \equiv y_i = 2 \left(\frac{P_{i-1} - z - w + w \sum_{j=0}^{i-1} P_j}{2 - 2z - w}\right),$$

where this recursion requires the definition $P_0 \equiv y_0 = 2$.

For stability to persist in the numerical solution, we must demand

$$|P_i(z, w)| < 2 \tag{6}$$

for all i , whenever $\lambda < 0$ and $\gamma \leq 0$, and $|y_i| = 2$ when $\lambda = \gamma = 0$. For a given stepsize h , this implies that $(z, w) = (h\lambda, h^2\gamma)$ is located in the third quadrant in the $z - w$ system.

We define the *stability region* S in the third quadrant as

$$S \equiv \{(z, w) \mid z < 0, w \leq 0 \text{ and } |P_i(z, w)| < 2 \text{ for all } i\} \cup \{(0, 0)\}.$$

The inclusion of $(z, w) = (0, 0)$ caters for the case $\lambda = \gamma = 0$.

At the time of writing, we are not in possession of an analytical proof that defines the boundary ∂S of S . Nevertheless, there is a useful numerical approach that we can adopt. We consider the region

$$R_I \equiv [-100, 0] \times [-100, 0]$$

in the $z - w$ plane. We choose a grid of 10^6 points $(z, w) \in R_I$, and we compute $|P_i(z, w)|$ for each of these points, for $i \in [1, 10^6]$. We determine, for each (z, w) , whether or not $|P_i(z, w)| > 2$ for any $i \in [1, 10^6]$. If not, we consider the point (z, w) to be *practically stable*. We have found that every single point in R_I that we considered was practically stable. This leads us to conjecture that all points in R_I are stable, so that, at the very least, $S = R_I$. Moreover, we speculate that S is actually given by the *entire* third quadrant, suggesting unconditional stability.

Such speculation notwithstanding, the practical approach to using our results is as follows: assume we have $\lambda \leq 0$ and $\gamma \leq 0$. Then the point $(z, w) = (\lambda, \gamma)$ is simply

$(z, w) = (h\lambda, h^2\gamma)$ with $h = 1$. If such point lies within R_I , then we expect the numerical solution, with $h = 1$, to be practically stable. It is likely to be inaccurate, but it will be stable. Even if we reduce h for the sake of accuracy, $(h\lambda, h^2\gamma)$ will still lie in R_I and practical stability will persist. If (λ, γ) lies outside R_I , then we simply choose h such that $(h\lambda, h^2\gamma) \in R_I$. Note that our definition of practical stability is tied to the maximal value of i that we considered (10^6). We expect that this large enough to cater for most practical calculations; if not, then the user can easily augment our results by checking the condition (6) for larger values for i .

3.2 Explicit case

Applying the explicit algorithm to the test equation yields

$$\begin{aligned} P_0 &= 2 \\ P_1(z, w) &= z + 2 \\ P_2(z, w) &= z^2 + \frac{zw}{2} + 2z + 2w + 2 \\ P_i(z, w) &\equiv 2 \left(\frac{(1 + z + \frac{w}{2}) P_{i-1} - z - w + w \sum_{j=0}^{i-2} P_j}{2} \right), \quad i \geq 3. \end{aligned}$$

Using a similar approach to that described above, we may construct a region R_E of practical stability for the explicit method, and we show this region in Figure 1. Also shown are curves, which we call *h-paths*, for various values of (λ, γ) . The *h-path* for (λ, γ) is the locus of points on the diagram for $(h\lambda, h^2\gamma)$, where $h \in [0, \infty]$. The *h-path* for (λ, γ) always passes through (λ, γ) - corresponding to $h = 1$ - and always terminates at the origin. It is clear that three of the *h-paths* shown (A, B and C) intersect R_E quite obviously; one of them (D), however, intersects R_E only near the origin. These *h-paths* indicate the effect of reducing h on the location of the point $(h\lambda, h^2\gamma)$. Recall, for stability, it is necessary to choose h such that $(h\lambda, h^2\gamma)$ lies within the stability region, and the *h-path* gives a clear idea of the range of values of h required to achieve that. For the *h-path* D that intersects R_E only near the origin, a very small value of h will be needed, particularly if λ and/or γ are strongly negative. For the other three *h-paths*, relatively larger values for h could be tolerated to achieve stability.

4 Error control

We assume the algorithms have a first-order error. Consequently, we can use Richardson extrapolation to achieve solutions of higher-order. We will not discuss this here, and the reader is referred to our previous work for the necessary detail [1][4]. In [1] we estimate the number of nodes needed for various tolerances when using a third-order solution. In this paper, we make similar estimates (in the next section) with reference to a fourth-order solution. In the notation of [1], we use $Y_i^4 - Y_i^5$ instead of $Y_i^3 - Y_i^5$ for error control. Again, the reader is referred to these previous papers for relevant detail.

5 Examples

We consider the same examples as used in [3], modified to suit our test equation. The parameters λ and γ are easily identified. The quantities N_1 and N_2 in Table 1 refer to the number of nodes (N in (2)) needed to achieve tolerances of $\varepsilon = 10^{-6}$ and $\varepsilon = 10^{-12}$, respectively, using the Richardson process described above. The stepsize can be found from $h = 10/(N - 1)$. The implicit algorithm yielded stable solutions for all the examples.

Table 1: Examples 1 – 3, implicit algorithm

#	IDE	x	N_1	N_2
1	$y' = -100(y - 1) - 0.1 \int_0^x y dt$	[0, 10]	1158	36606
2	$y' = -14(y - 1) - 15 \int_0^x y dt$	[0, 10]	207	6519
3	$y' = -0.1(y - 1) - 650 \int_0^x y dt$	[0, 10]	10044	317613

Results for the explicit algorithm are shown in Table 2. Here, N indicates the least number of nodes required for a stable solution, h_s is the corresponding stepsize and $(z, w) = (h_s \lambda, h_s^2 \gamma)$.

Table 2: explicit algorithm

#	N	h_s	(z, w)
1	505	0.0198	$(-1.98, 4 \times 10^{-5})$
2	72	0.1408	$(1.97, 0.3)$
3	9501	0.0011	$(-1.1 \times 10^{-5}, 7.8 \times 10^{-4})$

Note the very small stepsize needed for #3. This case corresponds to the h -path D in Figure 1 that is close to the vertical axis, and intersects the stability region only near the origin.

6 Conclusion

We have extended earlier work on the numerical solution of Volterra integro-differential equations by providing implicit and explicit versions of an Euler-type algorithm for a

kernel of general form. We have conducted a stability analysis. We have found that the implicit method is stable over a large region in the third quadrant of the stability space (and very possibly over the entire third quadrant), while the explicit method is stable over a relatively small region near the origin. Numerical examples with a suitable test equation support these findings.

References

- [1] J.S.C. Prentice, An Euler-type method for Volterra integro-differential equations, *arXiv.org* (Cornell University Library), 2023, 11p, [arXiv:2306.02547]
- [2] H. Brunner, *The numerical solution of Volterra equations*, North-Holland, New York (1986).
- [3] M.R. Crisci, E. Russo, A. Vecchio, Stability analysis of the de Hoog and Weiss implicit Runge-Kutta methods for the Volterra integral and integrodifferential equations, *Journal of Computational and Applied Mathematics*, 29 (1990) 329-341.
- [4] J.S.C. Prentice, Evaluating a double integral using Euler's method and Richardson extrapolation, *arXiv.org* (Cornell University Library), 2023, 17p, [arXiv:2305.07777]

7 Appendix A

7.1 Systems

When $n = 2$ in (1), we have the system

$$\begin{bmatrix} y_1' \\ y_2' \end{bmatrix} = \begin{bmatrix} y_2 \\ f(x, y_1) + \int_{x_0}^x K(x, y_1(t), t) dt \end{bmatrix}$$

and when $n = 3$, we have

$$\begin{bmatrix} y_1' \\ y_2' \\ y_3' \end{bmatrix} = \begin{bmatrix} y_2 \\ y_3 \\ f(x, y_1) + \int_{x_0}^x K(x, y_1(t), t) dt \end{bmatrix},$$

The initial values $y_1(x_0)$ and $y_2(x_0) = y_1'(x_0)$ must be specified for the first system, and $y_1(x_0), y_2(x_0) = y_1'(x_0)$ and $y_3(x_0) = y_2'(x_0)$ must be specified for the second system. Of course, analogous expressions exist for $n > 3$.

The general first-order system has the form

$$\begin{aligned} \begin{bmatrix} y'_1 \\ \vdots \\ y'_m \end{bmatrix} &= \begin{bmatrix} f_1(x, y_1, \dots, y_m) + \int_{x_0}^x K_1(x, y_1, \dots, y_m) dt \\ \vdots \\ f_m(x, y_1, \dots, y_m) + \int_{x_0}^x K_m(x, y_1, \dots, y_m) dt \end{bmatrix} \\ \Rightarrow \begin{bmatrix} y_{1,i+1} \\ \vdots \\ y_{m,i+1} \end{bmatrix} &= \begin{bmatrix} y_{1,i} + hG_1 \\ \vdots \\ y_{m,i} + hG_m \end{bmatrix}, \end{aligned}$$

where the forms of G_1 and G_m can be inferred. For this system, we can find the Jacobians

$$J_f \equiv \begin{bmatrix} \frac{\partial f_1}{\partial y_1} & \dots & \frac{\partial f_1}{\partial y_m} \\ \vdots & \ddots & \vdots \\ \frac{\partial f_m}{\partial y_1} & \dots & \frac{\partial f_m}{\partial y_m} \end{bmatrix} \quad \text{and} \quad J_K \equiv \begin{bmatrix} \frac{\partial K_1}{\partial y_1} & \dots & \frac{\partial K_1}{\partial y_m} \\ \vdots & \ddots & \vdots \\ \frac{\partial K_m}{\partial y_1} & \dots & \frac{\partial K_m}{\partial y_m} \end{bmatrix}.$$

Let $\{\lambda_1, \dots, \lambda_m\}$ denote the eigenvalues of J_f , and $\{\gamma_1, \dots, \gamma_m\}$ denote the eigenvalues of J_K . We form the pairs (λ_j, γ_j) . If $\lambda_j \leq 0$ and $\gamma_j \leq 0$, or $\text{Re } \lambda_j \leq 0$ and $\text{Re } \gamma_j \leq 0$ if the eigenvalues are complex, we write

$$(z, w) = (h\lambda_j, h^2\gamma_j) = \left(-h\sqrt{\lambda_j^*\lambda_j}, -h^2\sqrt{\gamma_j^*\gamma_j}\right).$$

8 Appendix B

To solve (3) for y_{i+1} we employ Newton's Method in the form

$$y_{i+1}^{k+1} = y_{i+1}^k - \frac{F(y_{i+1}^k)}{F'(y_{i+1}^k)},$$

where

$$\begin{aligned} F(y_{i+1}) &\equiv y_{i+1} - y_i - hf(x_{i+1}, y_{i+1}) \\ &\quad - \frac{h^2}{2} \left(\sum_{j=0}^{i+1} 2K(x_{i+1}, y_j, x_j) - K(x_{i+1}, y_0, x_0) - K(x_{i+1}, y_{i+1}, x_{i+1}) \right) \end{aligned}$$

and

$$F'(y_{i+1}) = \frac{dF(y_{i+1})}{dy_{i+1}} = 1 - h \frac{df(x_{i+1}, y_{i+1})}{dy_{i+1}} - \frac{h^2}{2} \frac{dK(x_{i+1}, y_{i+1}, x_{i+1})}{dy_{i+1}},$$

with initial value $y_{i+1}^0 = y_i$. We would generally expect second-order convergence for this method.

If we use

$$y_{i+1}^{k+1} = y_{i+1}^k - \frac{F(y_{i+1}^k)}{F'(y_{i+1}^k)} - \frac{F^2(y_{i+1}^k) F''(y_{i+1}^k)}{2 (F'(y_{i+1}^k))^3}$$

where

$$F''(y_{i+1}) = \frac{d}{dy_{i+1}} \frac{dF(y_{i+1})}{dy_{i+1}},$$

we may expect third-order convergence, which may improve the efficiency of the algorithm.

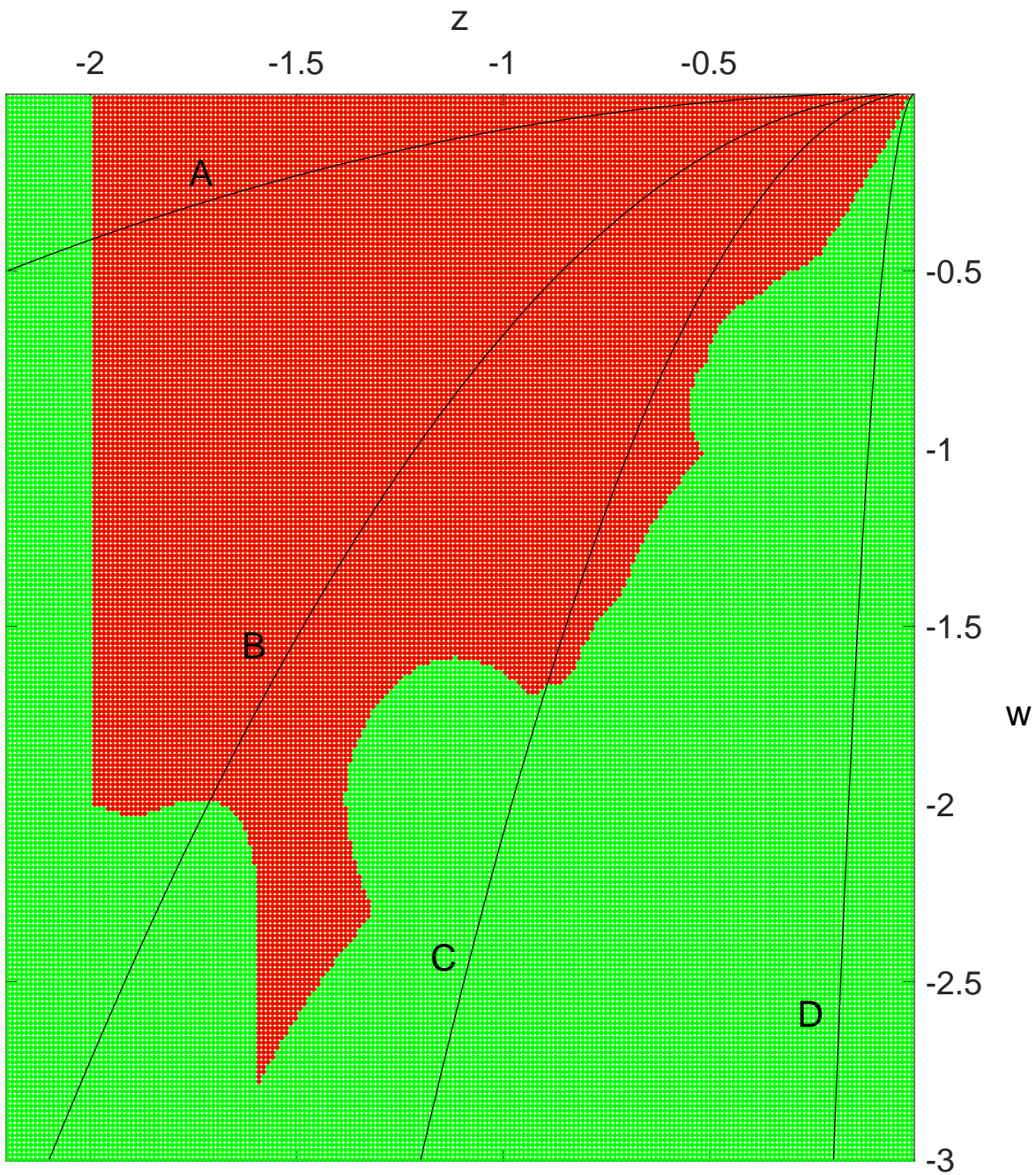


Figure 1

Stability region (red) for the explicit algorithm.
Various h -paths are also shown.